Received: 8 March 2021 | Revised: 26 June 2021 | Accepted: 5 August 2021

DOI: 10.1002/jnr.24946

RESEARCH ARTICLE

JOURNAL OF Neuroscience Research

Genetic variation in endocannabinoid signaling is associated with differential network-level functional connectivity in youth

Lucinda M. Sisk[1] | Kristina M. Rapuano[1] | May I. Conley[1] | Abigail S. Greene[2] | Corey Horien[2] | Monica D. Rosenberg[3] | Dustin Scheinost[4] | R. Todd Constable[2,4] | Charles E. Glatt[5] | B. J. Casey[1] | Dylan G. Gee[1]

[1]Department of Psychology, Yale University, New Haven, CT, USA

[2]Interdepartmental Neuroscience Program, Yale School of Medicine, New Haven, CT, USA

[3]Department of Psychology, University of Chicago, Chicago, IL, USA

[4]Department of Radiology and Biomedical Imaging, Yale School of Medicine, New Haven, CT, USA

[5]Department of Psychiatry, Weill Cornell Medicine, New York, NY, USA

Correspondence
Dylan G. Gee, Department of Psychology, Yale University, 2 Hillhouse Avenue, New Haven, CT 06511, USA.
Email: dylan.gee@yale.edu

Funding information
Brain and Behavior Research Foundation; National Institutes of Health; National Institute on Drug Abuse; National Science Foundation; National Institute of Mental Health; National Institute of General Medical Sciences; Society of Clinical Child and Adolescent Psychology; Jacobs Foundation

Abstract

The endocannabinoid system is an important regulator of emotional responses such as fear, and a number of studies have implicated endocannabinoid signaling in anxiety. The fatty acid amide hydrolase (FAAH) C385A polymorphism, which is associated with enhanced endocannabinoid signaling in the brain, has been identified across species as a potential protective factor from anxiety. In particular, adults with the variant FAAH 385A allele have greater fronto-amygdala connectivity and lower anxiety symptoms. Whether broader network-level differences in connectivity exist, and when during development this neural phenotype emerges, remains unknown and represents an important next step in understanding how the FAAH C385A polymorphism impacts neurodevelopment and risk for anxiety disorders. Here, we leveraged data from 3,109 participants in the nationwide Adolescent Brain Cognitive Development Study℠ (10.04 ± 0.62 years old; 44.23% female, 55.77% male) and a cross-validated, data-driven approach to examine associations between genetic variation and large-scale resting-state brain networks. Our findings revealed a distributed brain network, comprising functional connections that were both significantly greater (95% CI for p values = [<0.001, <0.001]) and lesser (95% CI for p values = [0.006, <0.001]) in A-allele carriers relative to non-carriers. Furthermore, there was a significant interaction between genotype and the summarized connectivity of functional connections that were greater in A-allele carriers, such that non-carriers with connectivity more similar to A-allele carriers (i.e., greater connectivity) had lower anxiety symptoms ($\beta = -0.041$, $p = 0.030$). These findings provide novel evidence of network-level changes in neural connectivity associated with genetic variation in endocannabinoid signaling and suggest that genotype-associated neural differences may emerge at a younger age than genotype-associated differences in anxiety.

KEYWORDS

anxiety, brain development, brain networks, endocannabinoid signaling, functional connectivity

Edited by Hilary Marusak and Cristina Ghiani. Reviewed by David Lydon-Staley, Danielle Gerhard, and Matt Hill.

1 | INTRODUCTION

Adolescence is a dynamic period of brain development, as well as a time when the incidence of mental health disorders peaks (Kessler et al., 2005; Lee et al., 2014). Anxiety disorders are among the most common psychiatric disorders that affect youth and frequently emerge during the adolescent period (Kessler et al., 2005). The endocannabinoid (eCB) system, a key modulator of emotion and stress response systems, has been implicated in the regulation of anxiety and fear-related behaviors across species (Lee et al., 2016; Lu & Mackie, 2016; Lutz et al., 2015; Mechoulam & Parker, 2013; Meyer et al., 2018).

Signaling of the eCB system in the brain occurs in part via the binding of a ligand, N-arachidonoylethanolamine (anandamide; AEA), to type 1 cannabinoid receptors (CB1; Jutras-Aswad et al., 2009; Katona & Freund, 2012; Lee et al., 2016). CB1 receptors are found throughout the brain and in multiple neuronal populations, most notably in GABAergic and glutamatergic neurons (Hill et al., 2007; Marsicano & Lutz, 1999; Meyer et al., 2018). AEA levels are regulated by fatty acid amide hydrolase (FAAH), which is an hydrolytic enzyme responsible for catabolizing intracellular AEA (Di Marzo, 2011). The FAAH C385A polymorphism (rs324420) is a common missense mutation that destabilizes the FAAH protein, resulting in reduced FAAH activity and increased levels of AEA (Sipe et al., 2002). The A-allele of this variant has been implicated in human populations and knock-in mouse models of FAAH C385A as an important genetic modulator of both structural and functional connectivity and anxiety. In adults, converging evidence across species has observed lower anxiety symptoms and greater resting-state fronto-amygdala connectivity in carriers of the A-allele variant, relative to non-carriers (Dincheva et al., 2015; Gärtner et al., 2019). Furthermore, recent work found that the strength of fronto-amygdala connectivity was inversely correlated with amygdalar binding of a FAAH probe, although this study did not find evidence for a relationship between fronto-amygdala connectivity and the FAAH C385A polymorphism (Green et al., 2021). Other studies have identified A-allele carriers as having lower threat-related amygdala reactivity (Hariri et al., 2009), as well as faster amygdala habituation to threat (Gunduz-Cinar et al., 2013). Several randomized controlled trials have also found that administration of a FAAH inhibitor in healthy adults resulted in improved fear extinction memory recall and decreased stress reactivity and negative affect (Mayo et al., 2020), improvement in anxiety symptoms for some individuals with social anxiety disorder (Schmidt et al., 2021), and moderation of activation in the amygdala, anterior cingulate, and insula (Paulus et al., 2020). Research in rodents has demonstrated that inhibition of FAAH in mice resulted in enhanced fear extinction learning (Gunduz-Cinar et al., 2013) and lower anxiety-like behaviors (Moreira et al., 2008). Together, this body of work provides strong evidence that reduced FAAH activity, and accompanying increases in AEA, modulate neural connectivity, and buffer anxiety.

During adolescence, the eCB system undergoes significant changes (Meyer et al., 2018). In particular, FAAH expression shows a marked increase across limbic and prefrontal regions of the brain in adolescent rodents, while AEA shows a concomitant decrease (Lee & Gorzalka, 2012; Lee et al., 2013). Furthermore, adolescence is a period of substantial neural maturation, including synaptic pruning (Spear, 2013), increases in myelination (Lebel & Deoni, 2018), and a shift in fronto-amygdala functional connectivity toward a more adult-like state (Gabard-Durnam et al., 2014; Gee et al., 2013). These shifts are paralleled by decreased fear extinction (Pattwell et al., 2012) and impaired contextual fear retrieval (Pattwell et al., 2011) during adolescence. Taken together, the convergence of these neurodevelopmental changes likely represents an adaptive state that supports burgeoning independence (Casey et al., 2015, 2016), but may also represent a sensitive window for the emergence of anxiety disorders (Lee et al., 2014; Powers & Casey, 2015).

Characterizing how functional connectivity and anxiety might vary during adolescence as a function of genetic variation in the FAAH C385A polymorphism remains an area of ongoing research. One cross-species study identified parallel evidence in mice and humans of an interaction between age and genotype, such that greater frontolimbic structural connectivity and decreased anxiety symptoms in A-allele carriers emerged only after age 12 (Gee et al., 2016). However, whether associations between FAAH genotype and functional connectivity parallel these previous findings in the structural domain is yet unknown. Furthermore, studies investigating the neural correlates of the FAAH C385A polymorphism have tended to focus on fronto-amygdala connections, given the well-established role of this circuitry in fear learning (Milad & Quirk, 2012). However, advances in analytic techniques, together with growing evidence that key processes such as fear learning likely occur via distributed networks that engage regions throughout the brain (Fraenz et al., 2020), pose the question of whether individuals with the FAAH C385A polymorphism are also characterized by global network-level differences.

In the present study, we aimed to examine associations between FAAH genotype and functional connectivity at rest in a large sample of youth participating in the Adolescent Brain Cognitive

Significance

In a large developmental sample, this work aims to examine brain connectivity associated with genetic variation in endocannabinoid signaling that has been identified as a protective factor against anxiety. We demonstrate that the fatty acid amide hydrolase C385A polymorphism is associated with differential functional network connectivity in youth and find a genotype-specific association between functional connectivity and anxiety symptoms. These findings suggest that genotype-associated changes in functional connectivity may precede the emergence of genotype-associated changes in anxiety symptoms, and may inform efforts to translate developmental neuroscience to optimize treatments for anxiety disorders.

Development Study℠ (ABCD Study®; Casey et al., 2018). We employed the network-based statistic (NBS; Zalesky et al., 2010), a data-driven approach, to identify functional networks that differ between youth with versus without the variant FAAH 385A allele (i.e., A-allele carriers vs. non-carriers). We hypothesized that network-level differences in resting-state functional connectivity would exist between genotypes, and that fronto-amygdala connections would emerge as having greater connectivity in A-allele carriers than non-carriers.

2 | MATERIALS AND METHODS

2.1 | Participants

Subjects were 3,109 youth (10.04 ± 0.62 years old; 44.23% female, 55.77% male) who participated in the ABCD Study. Using harmonized protocols (Casey et al., 2018) across 21 sites, this ongoing study has recruited over 11,000 children and aims to follow them for 10 years to characterize neurobiological and psychological development from late childhood to young adulthood. Parents provided written informed consent, and children provided verbal assent to participate in the study. Full details of ethics and oversight in the ABCD Study have been previously published (Clark et al., 2018). In the present study, our final sample (n = 3,109) was derived from a subset of individuals (N = 5,772) with fMRI data available through the ABCD Fast Track option as of April 2018 (Rapuano et al., 2020). Within this subset of 5,772 participants with fMRI data, we excluded individuals with excessive motion during all of their resting-state scans (mean framewise displacement ≥0.15 mm; n = 1,612), as well as individuals with autism spectrum disorder (n = 52), cerebral palsy (n = 2), epilepsy (n = 30), hemorrhage (n = 2), intellectual disability (n = 3), schizophrenia (n = 1), traumatic brain injury (n = 1), or who were missing data for covariates (n = 916). We also excluded participants whose genetics data did not pass quality inspection, as reported in the Known Issues with Data Release 3.0 (https://nda.nih.gov/edit_collection.html?id=2573; n = 44). Detailed demographic data including age, sex, race, ethnicity, maternal education, and family income can be found in Table 1. Further details about the neural and behavioral data collected as part of the ABCD Study can be found in the original descriptor papers (Barch et al., 2018; Casey et al., 2018).

2.2 | Genetic, demographic, and symptom data

Baseline measures of behavioral, genetic, and demographic variables were obtained through the NIMH Data Archive Release 3.0 (https://doi.org/10.15154/1519007). We used the DSM-oriented anxiety disorder symptom scale from the child behavior checklist (CBCL; Achenbach et al., 2003; Achenbach & Rescorla, 2001) to measure anxiety symptoms in this sample. For each participant, a raw total score was computed as a sum of their parent or guardian's responses to the 11 items that comprise the anxiety disorder symptom scale. We used the Shapiro–Wilk test for normality to determine whether these scores required log transformation. Anxiety disorder symptom scores were used to evaluate associations between symptoms, genotype, and network connectivity. Subject-level genotype information was obtained from the imputed genetics data, which statistically infers unobserved genotypes. These data were generated using genotyping calls from the Affymetrix Smokescreen array, using a previously described pipeline (Kendall et al., 2017).

2.3 | Resting-state data

Details of imaging parameters and acquisition have been previously published (Casey et al., 2018). Each participant underwent three to four 5-min runs of a resting-state functional scan. At Siemens sites, if framewise Integrated Real-time Motion Monitoring (FIRMM) software (Dosenbach et al., 2017) indicated that 12.5-min of usable data (Power et al., 2014) had been collected, the fourth resting-state run was not collected (Hagler et al., 2019). All resting-state data were acquired on either a Siemens, GE, or Phillips 3T MRI scanner, using a 32 channel head coil, on 27 scanners across 21 sites. Anatomical images were acquired using a T1w scan. Raw dicom images from the resting-state scans were obtained via ABCD Fast Track (April 2018) and preprocessed using BioImage Suite (Joshi et al., 2011). This pipeline has been previously described (Greene et al., 2018; Horien et al., 2019), and includes standard preprocessing steps such as slice time and motion correction, registration to the MNI template, regression of mean time courses in white matter, cerebrospinal fluid, and gray matter; and low-pass filtering. All non-linear registrations were visually inspected to confirm quality and accuracy. Finally, these data were parcellated using the Shen 368 functional connectivity atlas, and connectivity matrices were computed using Pearson correlations (Horien et al., 2019; Lacadie et al., 2008; Salehi et al., 2020; Shen et al., 2013; Yeo et al., 2011). Edges with negative correlations were retained in all analyses. One resting-state run was included in analysis for each participant. Mean framewise displacement was computed for each resting-state run, and subjects with at least one resting-state scan with mean framewise displacement under a motion threshold of 0.15mm were included in the analysis (Greene et al., 2018; Horien et al., 2018, 2019; Rapuano et al., 2020). For subjects with two or more scans for which the mean framewise displacement was under 0.15mm, we selected the run which had the lowest mean framewise displacement for use in the following analyses. Mean framewise displacement was also included as a fixed-effects covariate in our statistical modeling. Statistical analyses were performed in Python 3.7 (Rossum, 1995), while network visualizations were conducted using BioImage Suite Web (Papademetris et al., 2006) at multiple levels of analysis to aid interpretation (Horien et al., 2020).

2.4 | Analytic approach: Network-based statistic

We employed a Python implementation of the NBS toolbox (*BCTPY* version 0.5.0; https://github.com/aestrivex/bctpy) and

TABLE 1 Group comparisons for all variables were performed using Pearson's Chi-squared tests

Sample demographics				
Genotype	**Overall (*n* = 3,109)**	**AA/AC (*n* = 1,313)**	**CC (*n* = 1,796)**	***p* value**
Race				0.396[a]
Asian	46 (1.5%)	23 (1.8%)	23 (1.3%)	
Black	265 (8.5%)	115 (8.8%)	150 (8.4%)	
Multiracial	347 (11%)	150 (11%)	197 (11%)	
Native American	14 (0.5%)	7 (0.5%)	7 (0.4%)	
Other	80 (2.6%)	28 (2.1%)	52 (2.9%)	
Pacific Islander	1 (<0.1%)	0 (0%)	1 (<0.1%)	
White	2,331 (75%)	977 (74%)	1,354 (75%)	
Declined to answer	10 (0.3%)	3 (0.2%)	7 (0.3%)	
Do not know	16 (0.5%)	10 (0.8%)	6 (0.3%)	
Ethnicity				<0.001
Hispanic	508 (16%)	253 (19%)	255 (14%)	
Non-Hispanic	2,601 (84%)	1,060 (81%)	1,541 (86%)	
Sex				0.181
Female	1,375 (44%)	599 (46%)	776 (43%)	
Male	1,734 (56%)	714 (54%)	1,020 (57%)	
Age (months)				0.092
	121 (114–127)	121 (115–127)	121 (114–127)	
Family income (annual)				<0.001
<$50,000	705 (23%)	365 (28%)	340 (19%)	
$50,000–$100,000	943 (30%)	381 (29%)	562 (31%)	
$100,000–$200,000	1,042 (34%)	406 (31%)	636 (35%)	
$200,000+	419 (13%)	161 (12%)	258 (14%)	
Maternal education				<0.001
<HS	101 (3.2%)	63 (4.8%)	38 (2.1%)	
HS or GED	730 (23%)	322 (25%)	408 (23%)	
BA or AA	1,438 (46%)	601 (46%)	837 (47%)	
Masters	637 (20%)	249 (19%)	388 (22%)	
Doctoral	203 (6.5%)	78 (5.9%)	125 (7.0%)	

Note: The median and IQR values are reported for age.

Abbreviations: AA, Associate of Arts degree; BA, Bachelor of Arts degree; GED, General Educational Development test; HS, high school degree.

[a]Two categories (Declined to Answer and Pacific Islander) were omitted from the Chi-squared test for participant race, due to low endorsement.

1,000 iterations of 10-fold cross-validation (via *ScikitLearn*, version 0.21.3; Pedregosa et al., 2011) in order to perform a data-driven examination of network-level differences between A-allele carriers and non-carriers (Zalesky et al., 2010). The NBS is a procedure that is optimized to control for the vast number of multiple comparisons inherent to testing differences in every functional connection, or edge, by comparing the size of significant interconnected edges with random networks of interconnected edges (Zalesky et al., 2010). Essentially, the NBS performs two-tailed *t* tests for each edge in connectivity matrices between two groups of subjects. For each test, the *t*-statistic is thresholded at a given level, and edges meeting or surpassing that threshold form suprathreshold edges. The sizes of interconnected components within this suprathreshold matrix are then computed and stored. This process is then iterated *k* times, randomly permuting edges of the two groups and then counting the number of edges of the largest interconnected component. For each iteration, a *p* value indicating the likelihood of the identified component size relative to the null distribution is calculated.

2.5 | Analytic approach: Network identification

Our sample comprised 1,796 individuals with a homozygous CC genotype, and 1,313 individuals with an A-allele (genotype AC or AA). We applied 1,000 iterations of 10-fold cross-validation,

stratifying each fold such that an equal proportion of A-allele carriers and non-carriers were included in both training and testing folds (Scheinost et al., 2019). We then applied the NBS to each of the training folds, using a *t*-statistic threshold of $t = 2.58$, approximately equivalent to $p = 0.01$ for two-tailed tests. Within each of 9,000 training folds, we used $k = 100$ permutations to identify the significance of the network of edges differing between A-allele carriers and non-carriers relative to the null distribution.

2.6 | Analytic approach: Network confirmation

After using the NBS to identify network-level differences within each training fold, we applied the resulting adjacency matrix to the held-back testing fold, and separated the network into edges where A-allele carriers had greater connectivity than non-carriers, and edges where A-allele carriers had lesser connectivity than non-carriers. Next, we summed the connection strengths of each edge within both sets of connections (i.e., where A-allele carriers had greater connectivity than non-carriers, and where A-allele carriers had lesser connectivity than non-carriers) to obtain two network strength summary statistics (Finn et al., 2015; Rosenberg, Finn, et al., 2016; Rosenberg, Zhang, et al., 2016). All numeric-type variables (network summary statistics, age, genetic ancestry, and mean framewise displacement) were then *z*-scored so that models would produce standardized beta coefficents. Using mixed-effects models implemented via the *statsmodels* python package (version 0.12.2; Seabold & Perktold, 2010), we then evaluated the associations between network strength summary statistics and genotype within the testing fold while controlling for fixed effects of age, biological sex, pubertal status, family income, maternal education, ethnicity, genetic ancestry, and mean framewise displacement, as well as a nested random effect—specifically, a random intercept for family nested within scanner serial number (capturing both scanner and site effects). We opted to include family income, maternal education, and ethnicity within all models due to the fact that these variables differed significantly between A-allele carriers and non-carriers (Table 1). We calculated descriptive statistics for standardized beta coefficients, *t* statistics, and *p* values resulting from cross-validation. Finally, we collapsed across the adjacency matrices identified across 9,000 training folds such that edges that were selected in 75% or more folds were retained, while the rest were discarded. This yielded a final adjacency matrix that was then applied to the whole dataset for post hoc analyses examining associations between connectivity and anxiety symptoms.

2.7 | Clinical symptoms

Using mixed-effects modeling, we tested whether anxiety symptoms differed by genotype. In this model, we controlled for fixed effects of age, biological sex, pubertal status, family income, maternal education, ethnicity, genetic ancestry, and mean framewise displacement, as well as a nested random effect, specifically a random intercept for family nested within site.

2.8 | Post hoc analyses

After testing whether network-level differences were present between A-allele carriers and non-carriers, we next examined whether connectivity within this identified network was associated with anxiety symptoms across the whole sample. We applied the final adjacency matrix, retaining connections that were selected in 75% or more of the 9,000 training folds, to the whole dataset ($n = 3{,}109$). We again separated the network into edges where A-allele carriers had greater connectivity than non-carriers and edges where A-allele carriers had lesser connectivity than non-carriers. As before, we then summed the *r* values of these sets of edges to obtain network strength summary scores (Finn et al., 2015; Rosenberg, Finn, et al., 2016; Rosenberg, Zhang, et al., 2016). In order to examine associations between connectivity and symptoms, we then performed two analyses using mixed-effects models: first, we examined whether connectivity of either the set of edges where A-allele carriers had greater connectivity than non-carriers, or the set of edges where A-allele carriers had lesser connectivity than non-carriers, was associated with anxiety symptoms (controlling for fixed effects of age, biological sex, pubertal status, family income, maternal education, ethnicity, genetic ancestry, and mean framewise displacement, as well as a nested random effect, specifically a random intercept for family nested within scanner serial number). Second, we evaluated whether genotype moderated the association between connectivity of a given set of edges and anxiety symptoms (controlling for fixed effects of age, biological sex, pubertal status, family income, maternal education, ethnicity, genetic ancestry, and mean framewise displacement, as well as a nested random effect, specifically a random intercept for family nested within scanner serial number), such that connectivity was associated with symptoms in a genotype-specific manner.

2.9 | Examination of fronto-amygdala edges

Given robust evidence in the literature that increased fronto-amygdala connectivity is associated with reduced anxiety symptoms starting in adolescence, we tested whether fronto-amygdala edges were included within the network identified by NBS, and further, whether they were included in the set of edges where A-allele carriers had greater connectivity than non-carriers. In order to examine this within both sets of edges, we selected all edges that had at least one connection with a node corresponding to either the left or right amygdala (as defined in the Shen 368 atlas; Horien et al., 2019), so that all edges connected to bilateral amygdalae were retained. Additionally, we computed the number of bilateral amygdala edges

that would be expected at a chance level. As both the left and right amygdala nodes have 368 possible connections (with one possible duplicated edge across both matrices connecting left and right amygdala nodes), and matrices representing these connections are symmetrical, we determined the number of edges expected at chance levels by multiplying the overall proportion of edges selected by the network by 367.5.

3 | RESULTS

3.1 | Distribution of anxiety disorder symptoms scores

Application of the Shapiro–Wilk test for normality to the CBCL anxiety disorder symptoms scores determined that these scores were not normally distributed ($p < 0.001$). We thus applied a log transformation to this variable, which reduced skew from 1.66 to 0.29 and kurtosis from 3.36 to −0.99. All subsequent modeling examining associations between anxiety symptoms and other measures of interest used this log-transformed score.

3.2 | Identification of resting-state connectivity networks

As predicted, we identified a network across all training folds that differed significantly between A-allele carriers and non-carriers. This network included edges where A-allele carriers had greater connectivity compared to non-carriers, as well as lesser connectivity compared to non-carriers (across all folds, $p_{NBS} < 0.01$). Within the testing folds, results from mixed-effects models also demonstrated significant differences between genotypes among connections where A-allele carriers showed greater connectivity than non-carriers (95% CI for β coefficients = [0.565, 1.076]; 95% CI for t values = [5.315, 10.645]; 95% CI for p values = [<0.001, <0.001]), and among connections where A-allele carriers showed lesser connectivity than non-carriers (95% CI for β coefficients = [−0.275, −0.868]; 95% CI for t values = [−2.746, −8.532]; 95% CI for p values = [0.006, <0.001]). These identified sets of edges comprised distributed networks involving regions throughout the brain (Figure 1). Histograms illustrating the distribution of r values for edges where A-allele carriers had greater connectivity than non-carriers, and edges where A-allele carriers had lesser connectivity than non-carriers, can be found in Figure S1.

3.3 | Clinical symptoms

We did not observe a significant association between genotype and log-transformed anxiety symptom scores ($\beta = -0.031$, $t = -1.187$, $SD = 0.026$, $p = 0.235$).

3.4 | Post hoc analyses

After selecting only edges that had been identified in 75% or more of the testing folds, we retained a network containing 756 edges, approximately 0.011% of 67,528 possible connections, which was then applied to the full sample to evaluate associations between connectivity and log-transformed anxiety symptoms. Using mixed-effects models across the entire dataset, we found that there was no association between summary statistics for either the set of edges where A-allele carriers had greater connectivity than non-carriers and log-transformed anxiety symptoms ($\beta = -0.009$, $t = -0.630$, $SD = 0.014$, $p = 0.528$), or for the set of edges where A-allele carriers had lesser connectivity than non-carriers and log-transformed anxiety symptoms ($\beta = -0.003$, $t = -0.233$, $SD = 0.015$, $p = 0.823$). However, genotype significantly moderated the association between the summary statistic for connectivity of the set of edges where A-allele carriers had greater connectivity than non-carriers and log-transformed anxiety symptoms (Figure 2; $\beta = 0.083$, $t = 3.114$, $SD = 0.027$, $p = 0.002$). Whereas there was no association between connectivity of the set of edges where A-allele carriers had greater connectivity than non-carriers and log-transformed anxiety symptoms among A-allele carriers ($\beta = 0.038$, $t = 1.649$, $SD = 0.023$, $p = 0.099$), connectivity of the set of edges where A-allele carriers had greater connectivity than non-carriers was negatively associated with log-transformed anxiety symptoms among non-carriers ($\beta = -0.041$, $t = -2.167$, $SD = 0.019$, $p = 0.030$). Genotype also significantly moderated the association between the summary statistic for connectivity of the set of edges where A-allele carriers had lesser connectivity than non-carriers and log-transformed anxiety symptoms ($\beta = -0.061$, $t = -2.304$, $SD = 0.026$, $p = 0.021$). However, this association was not significant within either A-allele carriers ($\beta = -0.041$, $t = -1.756$, $SD = 0.023$, $p = 0.079$) or within non-carriers ($\beta = 0.023$, $t = 1.194$, $SD = 0.020$, $p = 0.232$).

3.5 | Examination of fronto-amygdala edges

In order to determine whether fronto-amygdala edges were included within the network identified by NBS, we filtered the sets of identified edges by node, retaining only edges within each set that were connected to either the left or right amygdala (Figure 3). The total number of amygdala-connected edges (7) exceeded the number we would expect to be identified within the NBS network based on chance (4). One of these edges was a fronto-amygdala connection, which was contained within the set of edges where A-allele carriers had lesser connectivity than non-carriers.

4 | DISCUSSION

Given a growing literature on developmental changes in endocannabinoid signaling related to anxiety, we applied a data-driven approach to examine differences in functional connectivity across the

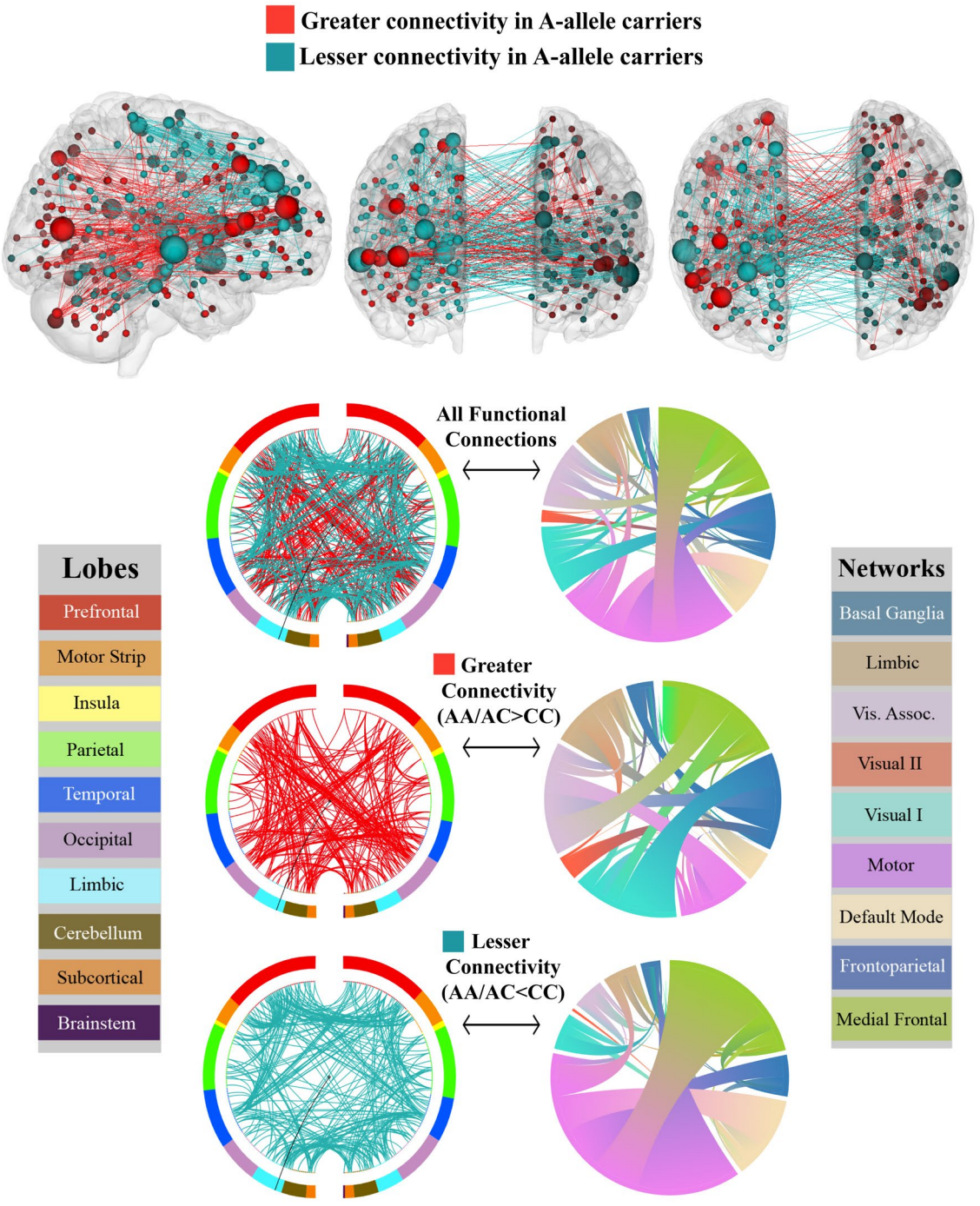

FIGURE 1 Network differences between A-allele carriers and non-carriers. Location and distribution of functional connections (edges) selected using the network-based statistic among lobes and functionally-defined networks. In the top panel, the red lines indicate edges connecting the red spheres, which represent nodes where A-allele carriers have greater connectivity than non-carriers. The blue lines indicate edges connecting the blue spheres, which represent nodes where non-carriers have greater connectivity than A-allele carriers. Nodes are sized according to degree (i.e., the number of edges connected to a given node). In the bottom left panel, the same nodes and edges are visualized in circle plots, in which nodes are grouped according to anatomic location. The top of the circle represents anterior; the bottom, posterior. The left half of the circle plot corresponds to the left hemisphere of the brain and the right half to the right hemisphere of the brain. A legend indicating the approximate anatomic "lobe" is shown to the left. In the chord plots in the bottom right panel, the edges are visualized by functional network to which each edge belongs. A legend indicating the corresponding functional networks is shown on the right. Vis. Assoc., Visual Association Network

brain associated with genetic variation in the FAAH C385A polymorphism among a large sample of youth. Our findings provide novel evidence that network-level differences in functional connectivity associated with the FAAH C385A polymorphism are present during preadolescence, and may precede the emergence of genotype-associated differences in anxiety symptoms. The identified network

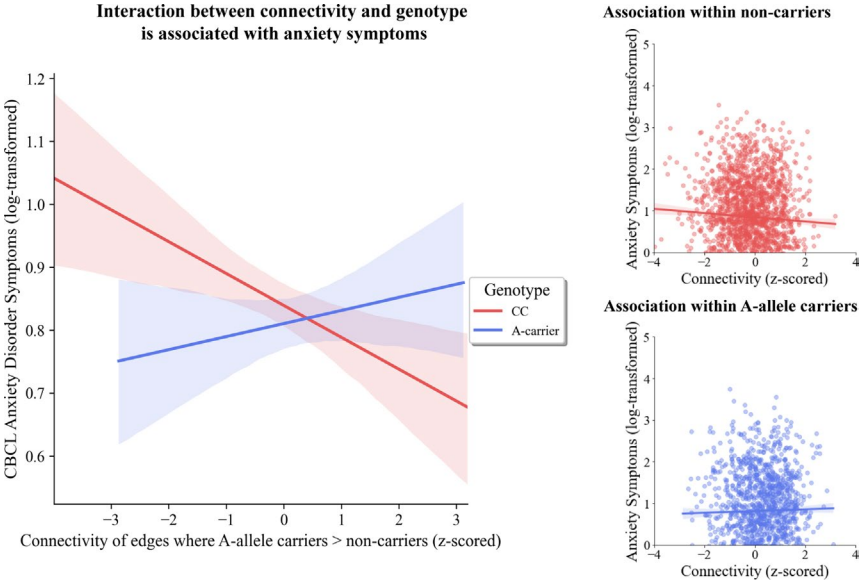

FIGURE 2 Associations between connectivity and anxiety symptoms. Genotype moderated the association between connectivity and log-transformed anxiety symptoms. The left plot depicts the interaction between genotype and strength of edges where A-allele carriers had greater connectivity than non-carriers. On the top right, non-carriers displayed a negative association between strength of edges where A-allele carriers had greater connectivity than non-carriers and log-transformed anxiety symptoms. On the bottom right, A-allele carriers did not display an association between strength of edges where A-allele carriers had greater connectivity than non-carriers and log-transformed anxiety symptoms. In order to most clearly illustrate both the interaction and the underlying data, we opted to show the interaction (*y*-axis zoomed in; left) and the associations between connectivity and anxiety within each genotype (right). Thus, the values on the *y*-axis in the zoomed-in plot on the left represent a smaller range of values than the *y*-axes in the plots on the right. In all plots, the *x*-axes represent the *z*-scored summed network connectivity statistic, representing the connectivity (or strength) of edges for which A-allele carriers had greater connectivity than non-carriers. See Figure S2 for rain cloud plots of raw CBCL Anxiety Disorder Symptoms scores

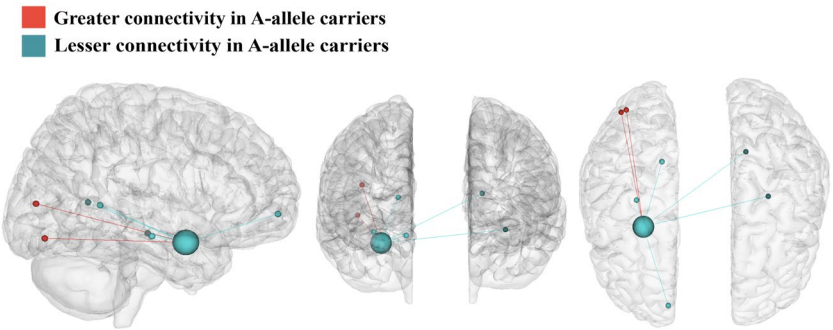

FIGURE 3 Amygdala-connected edges that differed between A-allele carriers and non-carriers. Glass brain visualization of all amygdala-connected edges that were retained within the network identified using the network-based statistic. Two amygdala-connected edges where A-allele carriers had greater connectivity than non-carriers were identified, while five edges where A-allele carriers had lesser connectivity than non-carriers were identified. All edges were connected to the right amygdala

involved a distributed set of regions, involved in all major functional networks across the brain (e.g., medial frontal, frontoparietal, motor, and visual networks). Moreover, non-carriers with connectivity more similar to A-allele carriers' connectivity (i.e., greater connectivity) showed decreased anxiety symptoms, suggesting a possible brain phenotype linking anxiety and the FAAH C385A genotype. This finding underscores the relation between brain connectivity and symptom emergence in the developing brain, and emphasizes the importance of a multimodal approach in examining associations between brain and behavioral phenotypes.

The network-based statistic approach used in this study allowed us to identify a broad network of functional connections that differ as a function of genetic variation in the FAAH C385A polymorphism, providing evidence that genotype-related changes extend beyond frontolimbic circuitry to regions involved in other primary functional networks of the brain. These findings highlight the distributed nature of neural processing (Finn et al., 2015; Greene et al., 2018; Rapuano et al., 2020; Rosenberg, Finn, et al., 2016), and support growing evidence that emotion processing, which is thought to be regulated in part by the endocannabinoid system,

involves many regions across the brain (Camacho et al., 2019; Saarimäki et al., 2016).

This robust detection of network-level differences in functional connectivity at rest in children ages 9–10 has important implications for our understanding of how alterations in endocannabinoid signaling relate to neural and behavioral changes during development. Developmentally specific decreases in FAAH activity and increases in AEA likely contribute to the timing of when genotype-related differences in functional connectivity emerge. Previous cross-species work has shown that greater structural frontolimbic connectivity and lower anxiety symptoms in A-allele carriers emerge around the transition to adolescence (Gee et al., 2016). The lack of differences in anxiety symptoms between A-allele carriers and non-carriers in the current study is consistent with past findings that anxiety symptoms did not differ by genotype prior to adolescence. The younger sample examined here did show network-level differences in functional connectivity at rest, suggesting that changes in endocannabinoid signaling associated with genetic variation may shape functional connectivity prior to differences in structural connectivity. Previous work has also consistently observed greater connectivity specifically in frontolimbic circuitry in A-allele carriers by adulthood (Dincheva et al., 2015; Gärtner et al., 2019). Interestingly, the present analysis did not identify greater fronto-amygdala connectivity in A-allele carriers, which may be consistent with the theory that previously reported increases in frontolimbic connectivity and decreases in anxiety symptoms emerge at a later developmental stage. However, it is also possible that the connectivity differences observed in A-allele carriers in the current work may reflect an intermediate phenotype that is more closely linked to genotype than anxiety (Meyer-Lindenberg, 2009), or that genotype-related differences in anxiety that were observed in prior work may not have survived in larger samples.

Cross-species research has demonstrated that the presence of the FAAH C385A polymorphism, as well as pharmacologically induced FAAH inhibition, result in enhanced fear extinction learning, decreased autonomic stress response, decreased stress-related negative affect (Mayo et al., 2020), more rapid amygdala habituation to threat (Gunduz-Cinar et al., 2013; Hariri et al., 2009), and reduced anxiety levels (Dincheva et al., 2015; Gee et al., 2016; Schmidt et al., 2021). The clinical potential of FAAH inhibition is evident, and indeed, randomized controlled trials have been conducted in adults (Mayo et al., 2020; Paulus et al., 2020; Schmidt et al., 2021). Reduction in FAAH activity levels may confer protective effects for A-allele carriers as early as adolescence (Gee et al., 2016), but elucidating the complex interactions between neural development and genetic variation will be critical in order to optimize treatments based on developmental stage (Casey et al., 2015).

While this study enhances understanding of the neural changes that accompany the FAAH C385A polymorphism prior to adolescence, it will be important for future research to build upon various aspects of this research. Although we conducted this work using a subset of data from a large, nationwide study with a population-based sample (Compton et al., 2019; Garavan et al., 2018), it will be necessary to confirm results from this study through external validation (ideally in a dataset with an equal or larger, demographically diverse sample). Importantly, while large sample sizes provide increased statistical power to observe smaller effects, assessing clinical significance can be challenging (Anvari et al., 2021; Dick et al., 2020). As benchmarked via heuristics for standardized betas (Acock, 2008), in the current work we observed a large effect size for the association between genotype and connectivity greater for A-allele carriers than non-carriers, a moderate effect size for the association between genotype and connectivity lesser for A-allele carriers than non-carriers, and small effect sizes for the associations between connectivity and anxiety symptoms. Following up on these findings in a separate dataset and longitudinally may inform the extent to which they are clinically meaningful. In this study we examined only cross-sectional neuroimaging data from youth ages 9–10. Given that changes in neural circuitry and behavior during adolescence coincide with an increase in FAAH activity as endocannabinoid signaling shifts, it will be important to further explore how associations between genotype, neural connectivity, and symptoms fluctuate over the course of development. Such investigations with the release of future longitudinal ABCD data will provide insight into whether the patterns of connectivity described in this paper reflect a time-limited phenotype of brain connectivity during a period of significant change, or potentially a more stable alteration in connectivity that remains throughout adolescence, as well as whether the directionality of fronto-amygdala connectivity observed here persists. In addition, while the current findings suggest that the FAAH C385A polymorphism is associated with functional alterations in regions distributed across many networks in the brain, we anticipate that future work will be helpful for better understanding the cognitive and behavioral implications of such widespread, network-level differences. Finally, although neural and behavioral differences have been linked with the FAAH C385A polymorphism across species, more complex genetic dynamics beyond a single candidate gene likely shape these outcomes. In order to better characterize the impact of the FAAH polymorphism, it will be important to examine associations between functional connectivity and anxiety symptoms in the context of other potential genetic modulators of endocannabinoid signaling.

In conclusion, the present findings identified a large-scale functional network that differed among youth as a function of genetic variation in the FAAH C385A polymorphism. This study demonstrates the utility of data-driven methods in extending current knowledge about the neural circuitry related to the endocannabinoid system and development, and provides novel evidence of differences in functional connectivity associated with the FAAH C385A polymorphism that may be present prior to the emergence of differences in anxiety symptoms by genotype. Finally, this study lays the groundwork for future research to examine precise trajectories of functional connectivity and symptom development throughout adolescence, enhancing our understanding of how the FAAH C385A polymorphism may buffer against anxiety.

ACKNOWLEDGMENTS

This work was supported by funding from the National Science Foundation Graduate Research Fellowship Program award (NSF DGE-1752134) for LMS; the National Institute on Drug Abuse (U01DA041174) for BJC and DGG; the National Institutes of Health (NIH) Director's Early Independence Award (DP5OD021370), Brain & Behavior Research Foundation (NARSAD Young Investigator Award), Jacobs Foundation Early Career Research Fellowship, and The Society for Clinical Child and Adolescent Psychology (Division 53 of the American Psychological Association) Richard "Dick" Abidin Early Career Award and Grant for DGG; a Medical Scientist Training Program training grant (NIH NIGMS-T32GM007205) for CH and ASG; and a National Institute of Mental Health grant (R01MH121095) for DS and RTC. The funders had no role in study design, data collection and analysis, decision to publish, or preparation of the manuscript.

CONFLICT OF INTEREST

The authors report no conflict of interest.

AUTHOR CONTRIBUTIONS

Conceptualization, L.M.S., D.G.G., B.J.C., and C.E.G.; *Methodology*, L.M.S., K.M.R., M.D.R., M.I.C., A.S.G., C.H., D.S., and R.T.C.; *Investigation*, B.J.C., D.G.G., and M.I.C.; *Formal Analysis*, L.M.S.; *Writing – Original Draft*, L.M.S., K.M.R., M.I.C., A.S.G, C.H., M.D.R., D.S., R.T.C., C.E.G., B.J.C., and D.G.G.; *Writing – Review & Editing*, L.M.S. and D.G.G.; *Visualization*, L.M.S. and K.M.R.; *Supervision*, D.G.G., B.J.C., and R.T.C.; *Funding Acquisition*, L.M.S., D.G.G., B.J.C., R.T.C., D.S., A.S.G., and C.H.

PEER REVIEW

The peer review history for this article is available at https://publons.com/publon/10.1002/jnr.24946.

DATA AVAILABILITY STATEMENT

Data used in the preparation of this article were obtained from the Adolescent Brain Cognitive Development℠ (ABCD) Study (https://abcdstudy.org), held in the NIMH Data Archive (NDA). This is a multisite, longitudinal study designed to recruit more than 10,000 children age 9–10 and follow them over 10 years into early adulthood. The ABCD Study® is supported by the National Institutes of Health and additional federal partners under award numbers U01DA041048, U01DA050989, U01DA051016, U01DA041022, U01DA051018, U01DA051037, U01DA050987, U01DA041174, U01DA041106, U01DA041117, U01DA041028, U01DA041134, U01DA050988, U01DA051039, U01DA041156, U01DA041025, U01DA041120, U01DA051038, U01DA041148, U01DA041093, U01DA041089, U24DA041123, U24DA041147. A full list of supporters is available at https://abcdstudy.org/federal-partners.html. A listing of participating sites and a complete listing of the study investigators can be found at https://abcdstudy.org/consortium_members/. ABCD consortium investigators designed and implemented the study and/or provided data but did not necessarily participate in analysis or writing of this report. This manuscript reflects the views of the authors and may not reflect the opinions or views of the NIH or ABCD consortium investigators. The ABCD data repository grows and changes over time. The ABCD data used in this report came from NDA Release 3.0 (https://doi.org/10.15154/1519007) and the ABCD Fast Track release (April 2018). The NDA Study for this project contains further details on the sample used here, and can be accessed at http://dx.doi.org/10.15154/1520940.

REFERENCES

Achenbach, T. M., Dumenci, L., & Rescorla, L. A. (2003). DSM-oriented and empirically based approaches to constructing scales from the same item pools. *Journal of Clinical Child & Adolescent Psychology*, *32*(3), 328–340. https://doi.org/10.1207/S15374424JCCP3203_02

Achenbach, T., & Rescorla, L. (2001). Manual for the ASEBA school-age forms & profiles: An integrated system of multi-informant assessment. *Youth & Families*. Retrieved from https://scholar.google.com/scholar_lookup?title=Manual+for+the+ASEBA+school-age+forms+&+profiles:+an+integrated+system+of+mult-informant+assessment&author=TM+Achenbach&author=LA+Rescorla&publication_year=2001&

Acock, A. C. (2008). *A gentle introduction to stata* (2nd ed.). Stata Press.

Anvari, F., Kievit, R., Lakens, D., Przybylski, A. K., Tiokhin, L., Wiernik, B. M., & Orben, A. (2021). *Evaluating the practical relevance of observed effect sizes in psychological research*. PsyArXiv. https://doi.org/10.31234/osf.io/g3vtr

Barch, D. M., Albaugh, M. D., Avenevoli, S., Chang, L., Clark, D. B., Glantz, M. D., Hudziak, J. J., Jernigan, T. L., Tapert, S. F., Yurgelun-Todd, D., Alia-Klein, N., Potter, A. S., Paulus, M. P., Prouty, D., Zucker, R. A., & Sher, K. J. (2018). Demographic, physical and mental health assessments in the adolescent brain and cognitive development study: Rationale and description. *Developmental Cognitive Neuroscience*, *32*, 55–66. https://doi.org/10.1016/j.dcn.2017.10.010

Camacho, M. C., Karim, H. T., & Perlman, S. B. (2019). Neural architecture supporting active emotion processing in children: A multivariate approach. *Neuroimage*, *188*, 171–180. https://doi.org/10.1016/j.neuroimage.2018.12.013

Casey, B. J., Cannonier, T., Conley, M. I., Cohen, A. O., Barch, D. M., Heitzeg, M. M., Soules, M. E., Teslovich, T., Dellarco, D. V., Garavan, H., Orr, C. A., Wager, T. D., Banich, M. T., Speer, N. K., Sutherland, M. T., Riedel, M. C., Dick, A. S., Bjork, J. M., Thomas, K. M., … Dale, A. M. (2018). The adolescent brain cognitive development (ABCD) study: Imaging acquisition across 21 sites. *Developmental Cognitive Neuroscience*, *32*, 43–54. https://doi.org/10.1016/j.dcn.2018.03.001

Casey, B. J., Galván, A., & Somerville, L. H. (2016). Beyond simple models of adolescence to an integrated circuit-based account: A commentary. *Developmental Cognitive Neuroscience*, *17*, 128–130. https://doi.org/10.1016/j.dcn.2015.12.006

Casey, B. J., Glatt, C. E., & Lee, F. S. (2015). Treating the developing versus developed brain: Translating preclinical mouse and human studies. *Neuron*, *86*(6), 1358–1368. https://doi.org/10.1016/j.neuron.2015.05.020

Clark, D. B., Fisher, C. B., Bookheimer, S., Brown, S. A., Evans, J. H., Hopfer, C., Hudziak, J., Montoya, I., Murray, M., Pfefferbaum, A., & Yurgelun-Todd, D. (2018). Biomedical ethics and clinical oversight in multisite observational neuroimaging studies with children and adolescents: The ABCD experience. *Developmental Cognitive Neuroscience*, *32*, 143–154. https://doi.org/10.1016/j.dcn.2017.06.005

Compton, W. M., Dowling, G. J., & Garavan, H. (2019). Ensuring the best use of data: The adolescent brain cognitive development study. *JAMA Pediatrics*, *173*(9), 809–810. https://doi.org/10.1001/jamapediatrics.2019.2081

Di Marzo, V. (2011). Endocannabinoid signaling in the brain: Biosynthetic mechanisms in the limelight. *Nature Neuroscience*, *14*(1), 9–15. https://doi.org/10.1038/nn.2720

Dick, A. S., Watts, A. L., Heeringa, S., Lopez, D. A., Bartsch, H., Fan, C. C., Palmer, C., Reuter, C., Marshall, A., Haist, F., Hawes, S., Nichols, T. E., Barch, D. M., Jernigan, T. L., Garavan, H., Grant, S., Pariyadath, V., Hoffman, E., Neale, M., … Thompson, W. K. (2020). Meaningful effects in the adolescent brain cognitive development study. *BioRxiv*, 2020.09.01.276451. https://doi.org/10.1101/2020.09.01.276451

Dincheva, I., Drysdale, A. T., Hartley, C. A., Johnson, D. C., Jing, D., King, E. C., Ra, S., Gray, J. M., Yang, R., DeGruccio, A. M., Huang, C., Cravatt, B. F., Glatt, C. E., Hill, M. N., Casey, B. J., & Lee, F. S. (2015). FAAH genetic variation enhances fronto-amygdala function in mouse and human. *Nature Communications*, *6*, 6395. https://doi.org/10.1038/ncomms7395

Dosenbach, N. U. F., Koller, J. M., Earl, E. A., Miranda-Dominguez, O., Klein, R. L., Van, A. N., Snyder, A. Z., Nagel, B. J., Nigg, J. T., Nguyen, A. L., Wesevich, V., Greene, D. J., & Fair, D. A. (2017). Real-time motion analytics during brain MRI improve data quality and reduce costs. *Neuroimage*, *161*, 80–93. https://doi.org/10.1016/j.neuroimage.2017.08.025

Finn, E. S., Shen, X., Scheinost, D., Rosenberg, M. D., Huang, J., Chun, M. M., Papademetris, X., & Constable, R. T. (2015). Functional connectome fingerprinting: Identifying individuals based on patterns of brain connectivity. *Nature Neuroscience*, *18*(11), 1664–1671. https://doi.org/10.1038/nn.4135

Fraenz, C., Metzen, D., Merz, C. J., Selpien, H., Friedrich, P., Ocklenburg, S., Axmacher, N., & Genç, E. (2020). Fear learning sculpts functional brain connectivity at rest beyond the traditional fear network in humans. *BioRxiv*, 2020.05.26.115840. https://doi.org/10.1101/2020.05.26.115840

Gabard-Durnam, L. J., Flannery, J., Goff, B., Gee, D. G., Humphreys, K. L., Telzer, E., Hare, T., & Tottenham, N. (2014). The development of human amygdala functional connectivity at rest from 4 to 23 years: A cross-sectional study. *Neuroimage*, *95*, 193–207. https://doi.org/10.1016/j.neuroimage.2014.03.038

Garavan, H., Bartsch, H., Conway, K., Decastro, A., Goldstein, R. Z., Heeringa, S., Jernigan, T., Potter, A., Thompson, W., & Zahs, D. (2018). Recruiting the ABCD sample: Design considerations and procedures. *Developmental Cognitive Neuroscience*, *32*, 16–22. https://doi.org/10.1016/j.dcn.2018.04.004

Gärtner, A., Dörfel, D., Diers, K., Witt, S. H., Strobel, A., & Brocke, B. (2019). Impact of FAAH genetic variation on fronto-amygdala function during emotional processing. *European Archives of Psychiatry and Clinical Neuroscience*, *269*(2), 209–221. https://doi.org/10.1007/s00406-018-0944-9

Gee, D. G., Gabard-Durnam, L. J., Flannery, J., Goff, B., Humphreys, K. L., Telzer, E. H., Hare, T. A., Bookheimer, S. Y., & Tottenham, N. (2013). Early developmental emergence of human amygdala–prefrontal connectivity after maternal deprivation. *Proceedings of the National Academy of Sciences of the United States of America*, *110*(39), 15638–15643. https://doi.org/10.1073/pnas.1307893110

Gee, D. G., Fetcho, R. N., Jing, D., Li, A., Glatt, C. E., Drysdale, A. T., Cohen, A. O., Dellarco, D. V., Yang, R. R., Dale, A. M., Jernigan, T. L., Lee, F. S., & Casey, B. J., & PING Consortium. (2016). Individual differences in frontolimbic circuitry and anxiety emerge with adolescent changes in endocannabinoid signaling across species. *Proceedings of the National Academy of Sciences of the United States of America*, *113*(16), 4500–4505. https://doi.org/10.1073/pnas.1600013113

Green, D. G. J., Kim, J., Kish, S. J., Tyndale, R. F., Hill, M. N., Strafella, A. P., Tong, J., McCluskey, T., Westwood, D. J., Houle, S., Lobaugh, N. J., & Boileau, I. (2021). Fatty acid amide hydrolase binding is inversely correlated with amygdalar functional connectivity: A combined positron emission tomography and magnetic resonance imaging study in healthy individuals. *Journal of Psychiatry & Neuroscience: JPN*, *46*(2), E238–E246. https://doi.org/10.1503/jpn.200010

Greene, A. S., Gao, S., Scheinost, D., & Constable, R. T. (2018). Task-induced brain state manipulation improves prediction of individual traits. *Nature Communications*, *9*(1), 1–13. https://doi.org/10.1038/s41467-018-04920-3

Gunduz-Cinar, O., MacPherson, K. P., Cinar, R., Gamble-George, J., Sugden, K., Williams, B., Godlewski, G., Ramikie, T. S., Gorka, A. X., Alapafuja, S. O., Nikas, S. P., Makriyannis, A., Poulton, R., Patel, S., Hariri, A. R., Caspi, A., Moffitt, T. E., Kunos, G., & Holmes, A. (2013). Convergent translational evidence of a role for anandamide in amygdala-mediated fear extinction, threat processing and stress-reactivity. *Molecular Psychiatry*, *18*(7), 813–823. https://doi.org/10.1038/mp.2012.72

Hagler, D. J., Hatton, S. N., Cornejo, M. D., Makowski, C., Fair, D. A., Dick, A. S., Sutherland, M. T., Casey, B. J., Barch, D. M., Harms, M. P., Watts, R., Bjork, J. M., Garavan, H. P., Hilmer, L., Pung, C. J., Sicat, C. S., Kuperman, J., Bartsch, H., Xue, F., … Dale, A. M. (2019). Image processing and analysis methods for the adolescent brain cognitive development study. *Neuroimage*, *202*, 116091. https://doi.org/10.1016/j.neuroimage.2019.116091

Hariri, A. R., Gorka, A., Hyde, L. W., Kimak, M., Halder, I., Ducci, F., Ferrell, R. E., Goldman, D., & Manuck, S. B. (2009). Divergent effects of genetic variation in endocannabinoid signaling on human threat- and reward-related brain function. *Biological Psychiatry*, *66*(1), 9–16. https://doi.org/10.1016/j.biopsych.2008.10.047

Hill, E. L., Gallopin, T., Férézou, I., Cauli, B., Rossier, J., Schweitzer, P., & Lambolez, B. (2007). Functional CB1 receptors are broadly expressed in neocortical GABAergic and glutamatergic neurons. *Journal of Neurophysiology*, *97*(4), 2580–2589. https://doi.org/10.1152/jn.00603.2006

Horien, C., Greene, A. S., Constable, R. T., & Scheinost, D. (2020). Regions and connections: Complementary approaches to characterize brain organization and function. *Neuroscientist*, *26*(2), 117–133. https://doi.org/10.1177/1073858419860115

Horien, C., Noble, S., Finn, E. S., Shen, X., Scheinost, D., & Constable, R. T. (2018). Considering factors affecting the connectome-based identification process: Comment on Waller et al. *Neuroimage*, *169*, 172–175. https://doi.org/10.1016/j.neuroimage.2017.12.045

Horien, C., Shen, X., Scheinost, D., & Constable, R. T. (2019). The individual functional connectome is unique and stable over months to years. *Neuroimage*, *189*, 676–687. https://doi.org/10.1016/j.neuroimage.2019.02.002

Joshi, A., Scheinost, D., Okuda, H., Belhachemi, D., Murphy, I., Staib, L. H., & Papademetris, X. (2011). Unified framework for development, deployment and robust testing of neuroimaging algorithms. *Neuroinformatics*, *9*(1), 69–84. https://doi.org/10.1007/s12021-010-9092-8

Jutras-Aswad, D., DiNieri, J. A., Harkany, T., & Hurd, Y. L. (2009). Neurobiological consequences of maternal cannabis on human fetal development and its neuropsychiatric outcome. *European Archives of Psychiatry and Clinical Neuroscience*, *259*(7), 395–412. https://doi.org/10.1007/s00406-009-0027-z

Katona, I., & Freund, T. F. (2012). Multiple functions of endocannabinoid signaling in the brain. *Annual Review of Neuroscience*, *35*, 529–558. https://doi.org/10.1146/annurev-neuro-062111-150420

Kendall, K. M., Rees, E., Escott-Price, V., Einon, M., Thomas, R., Hewitt, J., O'Donovan, M. C., Owen, M. J., Walters, J. T. R., & Kirov, G. (2017). Cognitive performance among carriers of pathogenic copy number variants: Analysis of 152,000 UK biobank subjects. *Biological Psychiatry*, *82*(2), 103–110. https://doi.org/10.1016/j.biopsych.2016.08.014

Kessler, R. C., Berglund, P., Demler, O., Jin, R., Merikangas, K. R., & Walters, E. E. (2005). Lifetime prevalence and age-of-onset distributions of DSM-IV disorders in the national comorbidity survey replication. *Archives of General Psychiatry*, *62*(6), 593–602. https://doi.org/10.1001/archpsyc.62.6.593

Lacadie, C. M., Fulbright, R. K., Rajeevan, N., Constable, R. T., & Papademetris, X. (2008). More accurate Talairach coordinates for

neuroimaging using non-linear registration. *Neuroimage*, *42*(2), 717–725. https://doi.org/10.1016/j.neuroimage.2008.04.240

Lebel, C., & Deoni, S. (2018). The development of brain white matter microstructure. *Neuroimage*, *182*, 207–218. https://doi.org/10.1016/j.neuroimage.2017.12.097

Lee, F. S., Heimer, H., Giedd, J. N., Lein, E. S., Šestan, N., Weinberger, D. R., & Casey, B. J. (2014). Adolescent mental health—Opportunity and obligation. *Science*, *346*(6209), 547–549. https://doi.org/10.1126/science.1260497

Lee, T.- T.-Y., & Gorzalka, B. B. (2012). Timing is everything: Evidence for a role of corticolimbic endocannabinoids in modulating hypothalamic–pituitary–adrenal axis activity across developmental periods. *Neuroscience*, *204*, 17–30. https://doi.org/10.1016/j.neuroscience.2011.10.006

Lee, T.- T.-Y., Hill, M. N., Hillard, C. J., & Gorzalka, B. B. (2013). Temporal changes in N-acylethanolamine content and metabolism throughout the peri-adolescent period. *Synapse*, *67*(1), 4–10. https://doi.org/10.1002/syn.21609

Lee, T.- T.-Y., Hill, M. N., & Lee, F. S. (2016). Developmental regulation of fear learning and anxiety behavior by endocannabinoids. *Genes, Brain, and Behavior*, *15*(1), 108–124. https://doi.org/10.1111/gbb.12253

Lu, H.-C., & Mackie, K. (2016). An introduction to the endogenous cannabinoid system. *Biological Psychiatry*, *79*(7), 516–525. https://doi.org/10.1016/j.biopsych.2015.07.028

Lutz, B., Marsicano, G., Maldonado, R., & Hillard, C. J. (2015). The endocannabinoid system in guarding against fear, anxiety and stress. *Nature Reviews Neuroscience*, *16*(12), 705–718. https://doi.org/10.1038/nrn4036

Marsicano, G., & Lutz, B. (1999). Expression of the cannabinoid receptor CB1 in distinct neuronal subpopulations in the adult mouse forebrain. *European Journal of Neuroscience*, *11*(12), 4213–4225. https://doi.org/10.1046/j.1460-9568.1999.00847.x

Mayo, L. M., Asratian, A., Lindé, J., Morena, M., Haataja, R., Hammar, V., Augier, G., Hill, M. N., & Heilig, M. (2020). Elevated anandamide, enhanced recall of fear extinction, and attenuated stress responses following inhibition of fatty acid amide hydrolase: A randomized, controlled experimental medicine trial. *Biological Psychiatry*, *87*(6), 538–547. https://doi.org/10.1016/j.biopsych.2019.07.034

Mechoulam, R., & Parker, L. A. (2013). The endocannabinoid system and the brain. *Annual Review of Psychology*, *64*, 21–47. https://doi.org/10.1146/annurev-psych-113011-143739

Meyer, H. C., Lee, F. S., & Gee, D. G. (2018). The role of the endocannabinoid system and genetic variation in adolescent brain development. *Neuropsychopharmacology*, *43*(1), 21–33. https://doi.org/10.1038/npp.2017.143

Meyer-Lindenberg, A. (2009). Neural connectivity as an intermediate phenotype: Brain networks under genetic control. *Human Brain Mapping*, *30*(7), 1938–1946. https://doi.org/10.1002/hbm.20639

Milad, M. R., & Quirk, G. J. (2012). Fear extinction as a model for translational neuroscience: Ten years of progress. *Annual Review of Psychology*, *63*(1), 129–151. https://doi.org/10.1146/annurev.psych.121208.131631

Moreira, F. A., Kaiser, N., Monory, K., & Lutz, B. (2008). Reduced anxiety-like behaviour induced by genetic and pharmacological inhibition of the endocannabinoid-degrading enzyme fatty acid amide hydrolase (FAAH) is mediated by CB1 receptors. *Neuropharmacology*, *54*(1), 141–150. https://doi.org/10.1016/j.neuropharm.2007.07.005

Papademetris, X., Jackowski, M. P., Rajeevan, N., DiStasio, M., Okuda, H., Constable, R. T., & Staib, L. H. (2006). Bioimage suite: An integrated medical image analysis suite: An update. *Insight Journal*, *2006*, 209.

Pattwell, S. S., Bath, K. G., Casey, B. J., Ninan, I., & Lee, F. S. (2011). Selective early-acquired fear memories undergo temporary suppression during adolescence. *Proceedings of the National Academy of Sciences of the United States of America*, *108*(3), 1182–1187. https://doi.org/10.1073/pnas.1012975108

Pattwell, S. S., Duhoux, S., Hartley, C. A., Johnson, D. C., Jing, D., Elliott, M. D., Ruberry, E. J., Powers, A., Mehta, N., Yang, R. R., Soliman, F., Glatt, C. E., Casey, B. J., Ninan, I., & Lee, F. S. (2012). Altered fear learning across development in both mouse and human. *Proceedings of the National Academy of Sciences of the United States of America*, *109*(40), 16318–16323. https://doi.org/10.1073/pnas.1206834109

Paulus, M. P., Stein, M. B., Simmons, A. N., Risbrough, V. B., Halter, R., & Chaplan, S. R. (2020). The effects of FAAH inhibition on the neural basis of anxiety-related processing in healthy male subjects: A randomized clinical trial. *Neuropsychopharmacology*, *46*(5), 1011–1019. https://doi.org/10.1038/s41386-020-00936-w

Pedregosa, F., Varoquaux, G., Gramfort, A., Michel, V., Thirion, B., Grisel, O., Blondel, M., Prettenhofer, P., Weiss, R., Dubourg, V., Vanderplas, J., Passos, A., Cournapeau, D., Brucher, M., Perrot, M., & Duchesnay, É. (2011). Scikit-learn: Machine learning in python. *Journal of Machine Learning Research*, *12*(85), 2825–2830.

Power, J. D., Mitra, A., Laumann, T. O., Snyder, A. Z., Schlaggar, B. L., & Petersen, S. E. (2014). Methods to detect, characterize, and remove motion artifact in resting state fMRI. *Neuroimage*, *84*, 320–341. https://doi.org/10.1016/j.neuroimage.2013.08.048

Powers, A., & Casey, B. J. (2015). The adolescent brain and the emergence and peak of psychopathology. *Journal of Infant, Child, and Adolescent Psychotherapy*, *14*(1), 3–15. https://doi.org/10.1080/15289168.2015.1004889

Rapuano, K. M., Rosenberg, M. D., Maza, M. T., Dennis, N. J., Dorji, M., Greene, A. S., Horien, C., Scheinost, D., Todd Constable, R., & Casey, B. J. (2020). Behavioral and brain signatures of substance use vulnerability in childhood. *Developmental Cognitive Neuroscience*, *46*, 100878. https://doi.org/10.1016/j.dcn.2020.100878

Rosenberg, M. D., Finn, E. S., Scheinost, D., Papademetris, X., Shen, X., Constable, R. T., & Chun, M. M. (2016). A neuromarker of sustained attention from whole-brain functional connectivity. *Nature Neuroscience*, *19*(1), 165–171. https://doi.org/10.1038/nn.4179

Rosenberg, M. D., Zhang, S., Hsu, W.-T., Scheinost, D., Finn, E. S., Shen, X., Constable, R. T., Li, C.-S.- R., & Chun, M. M. (2016). Methylphenidate modulates functional network connectivity to enhance attention. *Journal of Neuroscience*, *36*(37), 9547–9557. https://doi.org/10.1523/JNEUROSCI.1746-16.2016

Rossum, G. (1995). *Python reference manual* [Technical Report]. CWI (Centre for Mathematics and Computer Science).

Saarimäki, H., Gotsopoulos, A., Jääskeläinen, I. P., Lampinen, J., Vuilleumier, P., Hari, R., Sams, M., & Nummenmaa, L. (2016). Discrete neural signatures of basic emotions. *Cerebral Cortex*, *26*(6), 2563–2573. https://doi.org/10.1093/cercor/bhv086

Salehi, M., Greene, A. S., Karbasi, A., Shen, X., Scheinost, D., & Constable, R. T. (2020). There is no single functional atlas even for a single individual: Functional parcel definitions change with task. *Neuroimage*, *208*, 116366. https://doi.org/10.1016/j.neuroimage.2019.116366

Scheinost, D., Noble, S., Horien, C., Greene, A. S., Lake, E. M. R., Salehi, M., Gao, S., Shen, X., O'Connor, D., Barron, D. S., Yip, S. W., Rosenberg, M. D., & Constable, R. T. (2019). Ten simple rules for predictive modeling of individual differences in neuroimaging. *Neuroimage*, *193*, 35–45. https://doi.org/10.1016/j.neuroimage.2019.02.057

Schmidt, M. E., Liebowitz, M. R., Stein, M. B., Grunfeld, J., Van Hove, I., Simmons, W. K., Van Der Ark, P., Palmer, J. A., Saad, Z. S., Pemberton, D. J., Van Nueten, L., & Drevets, W. C. (2021). The effects of inhibition of fatty acid amide hydrolase (FAAH) by JNJ-42165279 in social anxiety disorder: A double-blind, randomized, placebo-controlled proof-of-concept study. *Neuropsychopharmacology*, *46*(5), 1004–1010. https://doi.org/10.1038/s41386-020-00888-1

Seabold, S., & Perktold, J. (2010). Statsmodels: Econometric and statistical modeling with python. In *Python in Science Conference*, (pp. 92–96). https://doi.org/10.25080/Majora-92bf1922-011

Shen, X., Tokoglu, F., Papademetris, X., & Constable, R. T. (2013). Groupwise whole-brain parcellation from resting-state fMRI data for

network node identification. *Neuroimage*, *82*, 403–415. https://doi.org/10.1016/j.neuroimage.2013.05.081

Sipe, J. C., Chiang, K., Gerber, A. L., Beutler, E., & Cravatt, B. F. (2002). A missense mutation in human fatty acid amide hydrolase associated with problem drug use. *Proceedings of the National Academy of Sciences of the United States of America*, *99*(12), 8394–8399. https://doi.org/10.1073/pnas.082235799

Spear, L. P. (2013). Adolescent neurodevelopment. *Journal of Adolescent Health*, *52*(2), S7–S13. https://doi.org/10.1016/j.jadohealth.2012.05.006

Yeo, B. T., Krienen, F. M., Sepulcre, J., Sabuncu, M. R., Lashkari, D., Hollinshead, M., Roffman, J. L., Smoller, J. W., Zöllei, L., Polimeni, J. R., Fischl, B., Liu, H., & Buckner, R. L. (2011). The organization of the human cerebral cortex estimated by intrinsic functional connectivity. *Journal of Neurophysiology*, *106*(3), 1125–1165. https://doi.org/10.1152/jn.00338.2011

Zalesky, A., Fornito, A., & Bullmore, E. T. (2010). Network-based statistic: Identifying differences in brain networks. *Neuroimage*, *53*(4), 1197–1207. https://doi.org/10.1016/j.neuroimage.2010.06.041

SUPPORTING INFORMATION

Additional supporting information may be found online in the Supporting Information section.

FIGURE S1 Histogram distributions of network summary statistics (summed correlation *r* values) for edges where A-allele carriers had greater connectivity than non-carriers (left) and edges where A-allele carriers had lesser connectivity than non-carriers (right). For edges where A-allele carriers had greater connectivity than non-carriers, the summed *r* values were less negative for A-allele carriers than for non-carriers. For edges where A-allele carriers had lesser connectivity than non-carriers, the summed r values were less positive than for non-carriers

FIGURE S2 Distribution of raw CBCL anxiety disorder symptoms scores, plotted by genotype

Transparent Peer Review Report

How to cite this article: Sisk, L. M., Rapuano, K. M., Conley, M. I., Greene, A. S., Horien, C., Rosenberg, M. D., Scheinost, D., Constable, R. T., Glatt, C. E., Casey, B. J., & Gee, D. G. (2021). Genetic variation in endocannabinoid signaling is associated with differential network-level functional connectivity in youth. *Journal of Neuroscience Research*, 00, 1–13. https://doi.org/10.1002/jnr.24946